

Drabon, N., and Lowe, D.R., 2021, Progressive accretion recorded in sedimentary rocks of the 3.28–3.23 Ga Fig Tree Group, Barberton Greenstone Belt: GSA Bulletin, <https://doi.org/10.1130/B35973.1>.

Supplemental Material

Supplemental File S1. Additional Figures.

Figure S1. [A] Stratigraphic sections and lithofacies associations of the Sheba, Ulundi, and Mapepe Formation in the Northern and West Central Domains after Lowe and Nocita (1999), Condie et al. (1970), Nocita (1990), and Nocita and Lowe (1991). [B] Stratigraphic sections and lithofacies associations of the Mapepe Formation in the Southern and East-Central Domains after Lowe and Nocita (1999), Zentner (2014), Harrington (2017), and Drabon et al. (2019). S2 and S3 spherule beds were used as datums; in their absence, radiometric dates from tuff allow correlation. Lithofacies are not connected between belts because direct correlation is unclear. The Inyoka Fault marks a boundary between the ND and the WCD, Mbema Fault marks the boundary between the WCD and ECD. Smaller faults between structural belts were omitted for clarity. Correlations between spherule layers are based on tracing surface outcrop (solid lines) and approximate correlations based on age constraints (dashed lines). Depositional ages marked as (*) are from zircons in tuffs or reworked tuffs. Relevant maximum depositional ages from detrital zircons in sandstones are marked as (**). Correlations based on detrital zircon age constraints should be regarded as uncertain.

Figure S2. Igneous zircon probability density plots with weighted mean ages of the [A] volcanoclastic rocks of the Auber Villiers Formation and [B] Fig Tree shallow intrusive rocks.

Figure S3. Cr/Zr ratio of samples with stratigraphic control. Samples from Eastern Barite Valley and Manzimnyama Syncline are from the BARB5 and BARB4 drill cores, respectively, hence the stratigraphic height is measured in core depth. Samples from Umbaumba sequence are from Hofmann (2005) and samples from the Mlumati Syncline from Stoll et al. (2021). All structural belts represent the Mapepe Formation unless indicated. Note the changes in scale on both axes.

Figure S4. Th/Sc ratio of samples with stratigraphic control. Samples from Eastern Barite Valley and Manzimnyama Syncline are from the BARB5 and BARB4 drill cores, respectively, hence the stratigraphic height is measured in core depth. Samples from Umbaumba sequence are from Hofmann (2005) and samples from the Mlumati Syncline from Stoll et al. (2021). All structural belts represent the Mapepe Formation unless indicated. Note the changes in scale on both axes.

Figure S5. LaN/YbN ratio of samples with stratigraphic control. Samples from Eastern Barite Valley and Manzimnyama Syncline are from the BARB5 and BARB4 drill cores, respectively, hence the stratigraphic height is measured in core depth. Samples from Umbaumba sequence are from Hofmann (2005) and samples from the Mlumati Syncline from Stoll et al. (2021). Note the changes in scale on both axes.

Supplemental File S2. List of dated tuffs of the Fig Tree Group.

Supplemental File S3. U-Pb geochronological data.

Supplemental File S4. Mudstone geochemical data.

REFERENCES CITED (Supplemental File S2)

- Byerly, G.R., Krisner, A., Lowe, D.R., Todt, W., Walsh, M.M., Kröner, A., Lowe, D.R., Todt, W., and Walsh, M.M., 1996, Prolonged magmatism and time constraints for sediment deposition in the early Archean Barberton greenstone belt: Evidence from the Upper Onverwacht and Fig Tree groups: *Precambrian Research*, v. 78, p. 125–138, [https://doi.org/10.1016/0301-9268\(95\)00073-9](https://doi.org/10.1016/0301-9268(95)00073-9).
- de Ronde, C.E.J., Kamo, S., Davis, D.W., de Wit, M.J., and Spooner, E.T.C., 1991b, Field, geochemical and U-Pb isotopic constraints from hypabyssal felsic intrusions within the Barberton greenstone belt, South Africa: Implications for tectonics and the timing of gold mineralization: *Precambrian Research*, v. 49, p. 261–280, [https://doi.org/10.1016/0301-9268\(91\)90037-B](https://doi.org/10.1016/0301-9268(91)90037-B).
- Heubeck, C., Engelhardt, J., Byerly, G.R., Zeh, A., Sell, B., Luber, T., and Lowe, D.R., 2013, Timing of deposition and deformation of the Moodies Group (Barberton Greenstone Belt, South Africa): Very-high-resolution of Archaean surface processes: *Precambrian Research*, v. 231, p. 236–262, <https://doi.org/10.1016/j.precamres.2013.03.021>.
- Kamo, S.L., and Davis, D.W., 1994, Reassessment of Archean crustal development in the Barberton Mountain Land, South Africa, based on U-Pb dating: *Tectonics*, v. 13, p. 167–192, <https://doi.org/10.1029/93TC02254>.
- Kohler, E.A. and Anhaeusser, C.R., 2002, Geology and geodynamic setting of Archaean silicic metavolcaniclastic rocks of the Bien Venue Formation, Fig Tree Group, northeast Barberton greenstone belt, South Africa: *Precambrian Research*, v. 116, p. 199-235. [https://doi.org/10.1016/S0301-9268\(02\)00021-9](https://doi.org/10.1016/S0301-9268(02)00021-9).
- Kröner, A., Byerly, G.R., and Lowe, D.R., 1991, Chronology of early Archaean granite-greenstone evolution in the Barberton Mountain Land, South Africa, based on precise dating by single zircon evaporation: *Earth and Planetary Science Letters*, v. 103, p. 41–54, [https://doi.org/10.1016/0012-821X\(91\)90148-B](https://doi.org/10.1016/0012-821X(91)90148-B).
- Lowe, D.R., Byerly, G.R., and Kyte, F.T., 2014, Recently discovered 3.42–3.23 Ga impact layers, Barberton belt, South Africa: 3.8 Ga detrital zircons, Archean impact history, and tectonic implications: *Geology*, v. 42, p. 747–750, <https://doi.org/10.1130/G35743.1>.

1 **Data Repository File DR1 for**

2 **Progressive accretion recorded in sedimentary rocks of the 3.28-**

3 **3.23 Ga Fig Tree Group, Barberton Greenstone Belt**

4 **Nadja Drabon^{1,2*} and Donald R. Lowe²**

5 *¹Department of Earth and Planetary Sciences, Harvard University, 24 Oxford St., Rm 367-368; Cambridge,*
6 *MA 02138, USA*

7 *²Department of Geological Sciences, Stanford University, 450 Serra Mall, Bldg. 320, Rm. 118, Stanford,*
8 *CA 94305-2115, USA*

9 ** Corresponding author: ndrabon@fas.harvard.edu*

10

11

12

13

14

15

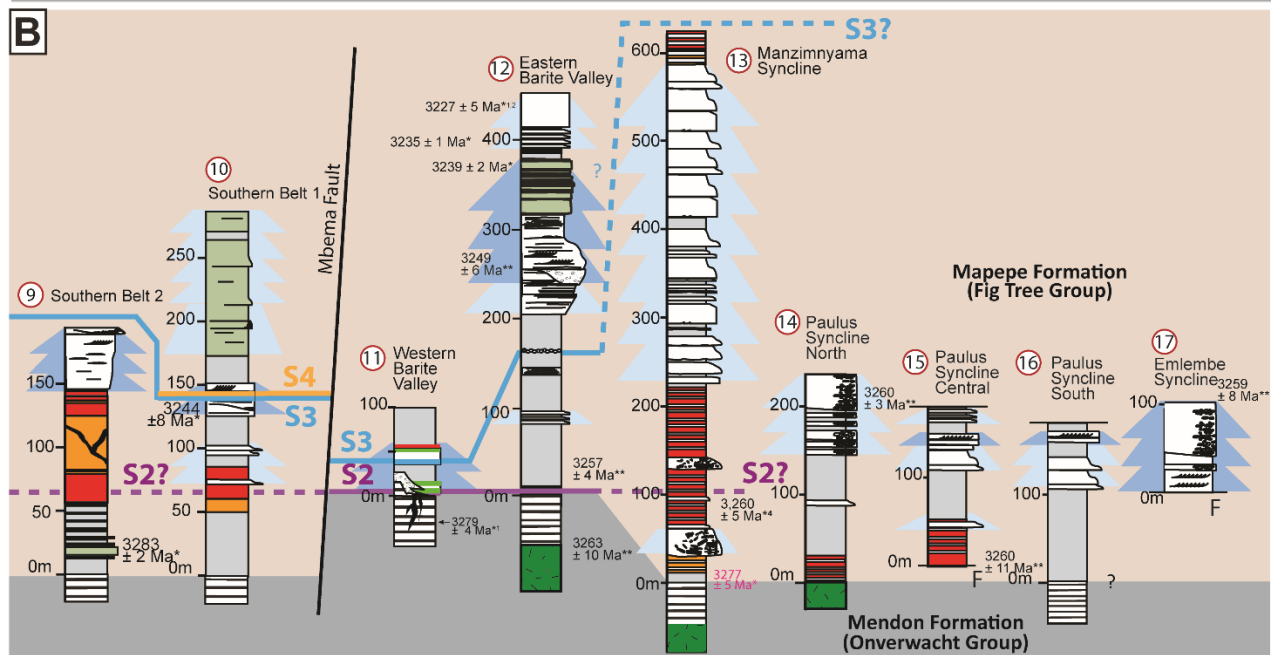
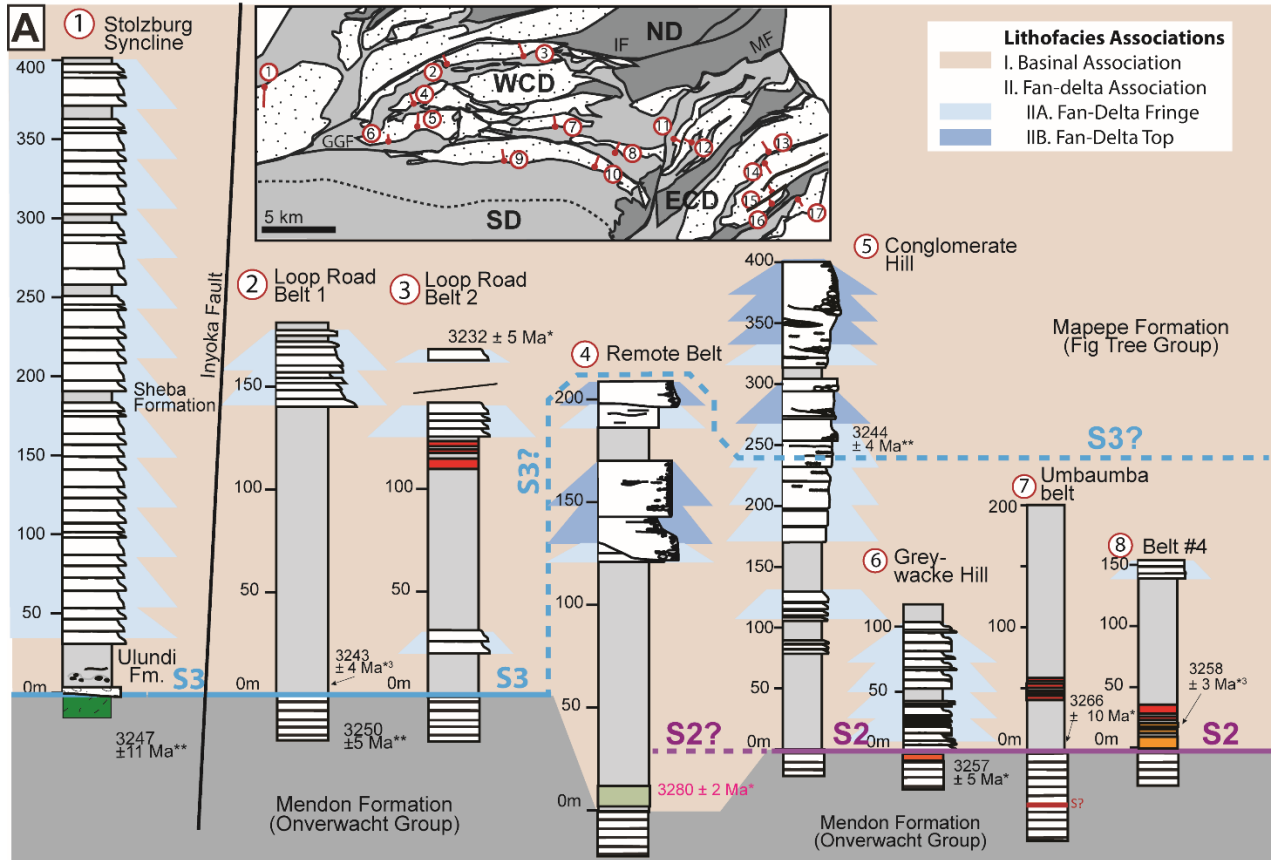
16

17

18

19

20 **Supplementary Figure 1:** [A] Stratigraphic sections and lithofacies associations of the Sheba, Ulundi,
21 and Mapepe Formation in the Northern and West Central Domains after Lowe and Nocita (1999), Condie
22 et al. (1970), Nocita (1990), and Nocita and Lowe (1991). [B] Stratigraphic sections and lithofacies
23 associations of the Mapepe Formation in the Southern and East-Central Domains after Lowe and Nocita
24 (1999), Zentner (2014), Harrington (2017), and Drabon et al. (2019). S2 and S3 spherule beds were used
25 as datums; in their absence, radiometric dates from tuff allow correlation. Lithofacies are not connected
26 between belts because direct correlation is unclear. The Inyoka Fault marks a boundary between the ND
27 and the WCD, Mbema Fault marks the boundary between the WCD and ECD. Smaller faults between
28 structural belts were omitted for clarity. Correlations between spherule layers are based on tracing surface
29 outcrop (solid lines) and approximate correlations based on age constraints (dashed lines). Depositional
30 ages marked as (*) are from zircons in tuffs or reworked tuffs. Relevant maximum depositional ages from
31 detrital zircons in sandstones are marked as (**). Correlations based on detrital zircon age constraints
32 should be regarded as uncertain.



Siliciclastic Sediments

- Mudstone
- Sandstone
- Conglomerate

Orthochemical Sediments

- Banded Iron Formation
- Banded Ferruginous Chert
- Black and White Banded Cherts

Volcanic Rocks

- Rhyolitic to dacitic volcaniclastic sediment
- Komatiite

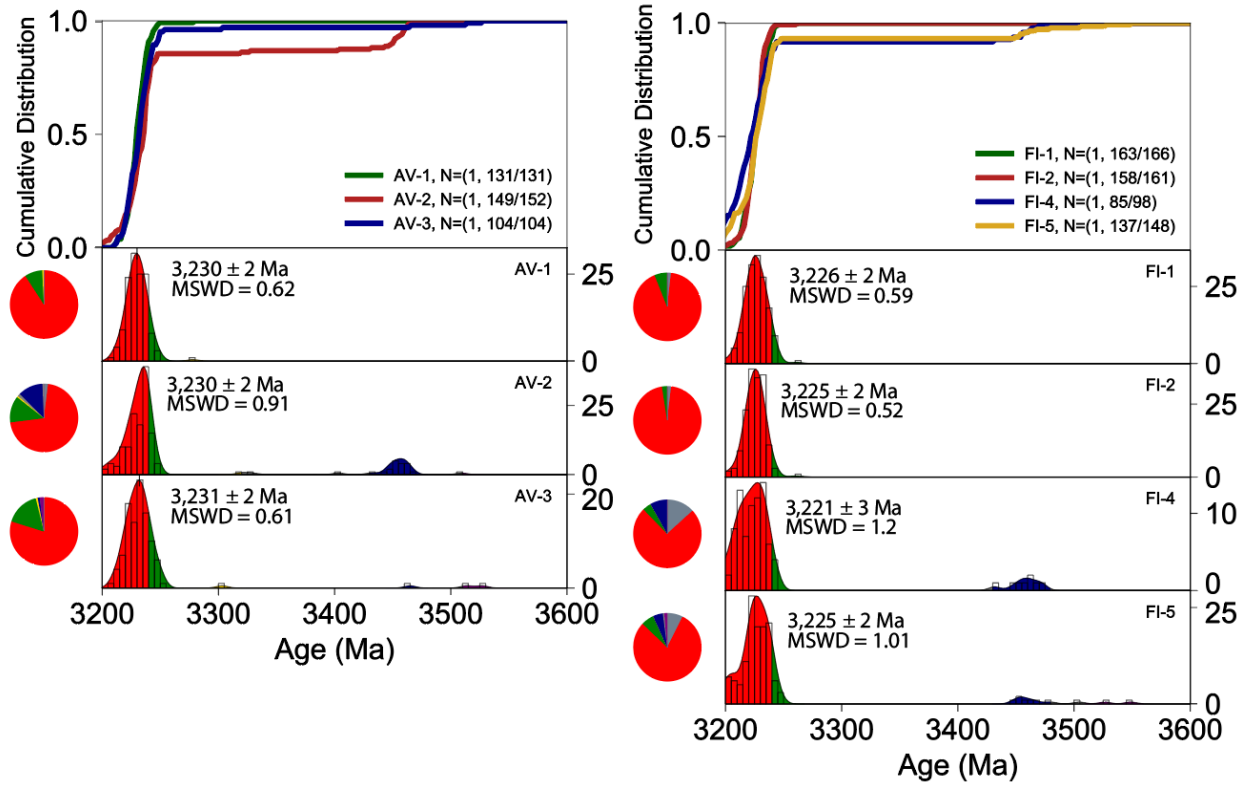
Sedimentary structures

- Cross-bedding
- Cross-lamination
- Horizontal lamination
- Soft-sediment deformation
- Reworked mud chips
- Mudcracks
- Pebble strings

* depositional age
** maximum depositional age

34 **Supplementary Figure 2:** Igneous zircon probability density plots with weighted mean ages of the [A]
35 volcaniclastic rocks of the Auber Villiers Formation and [B] Fig Tree shallow intrusive rocks.

36

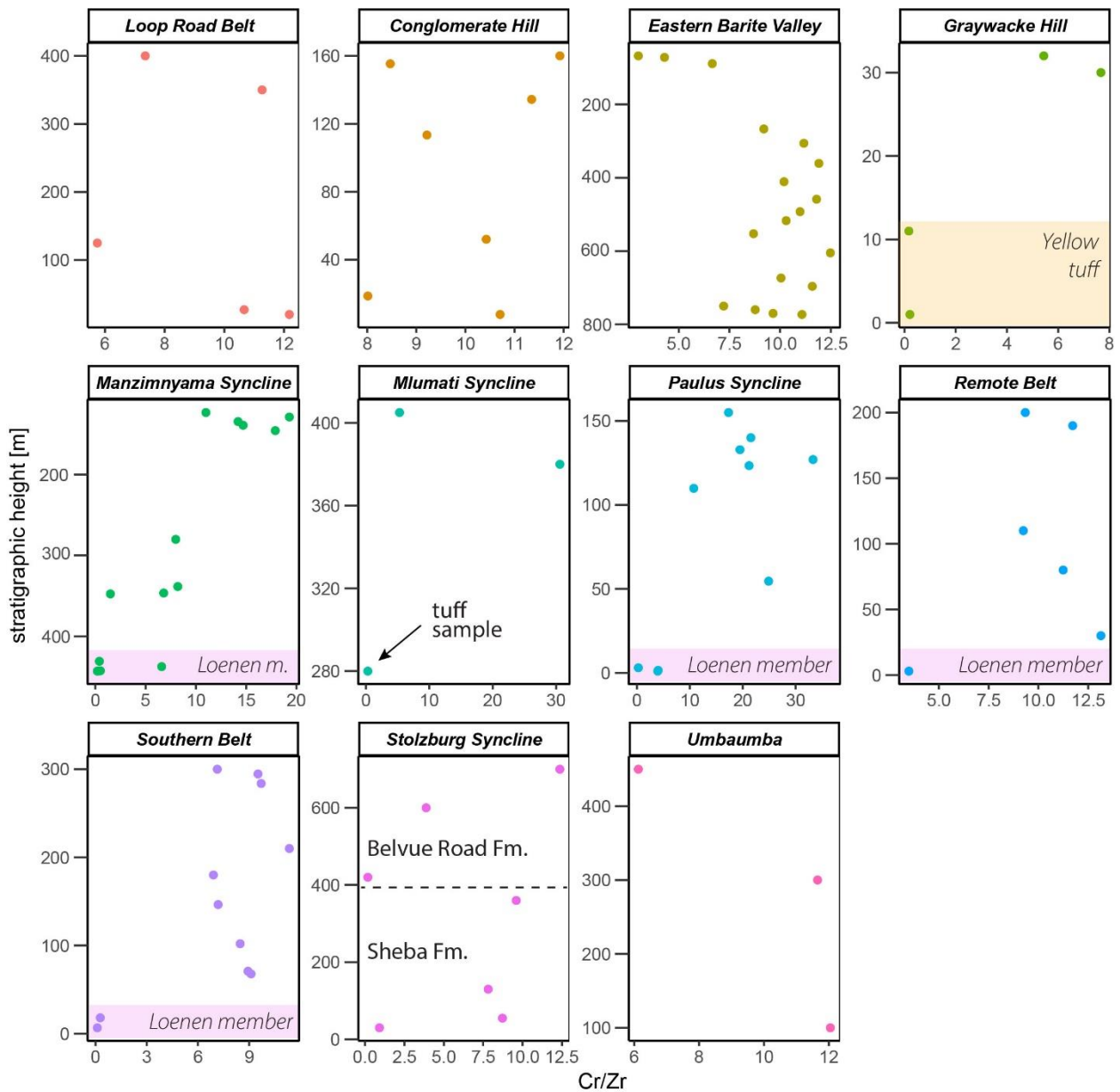


37

38

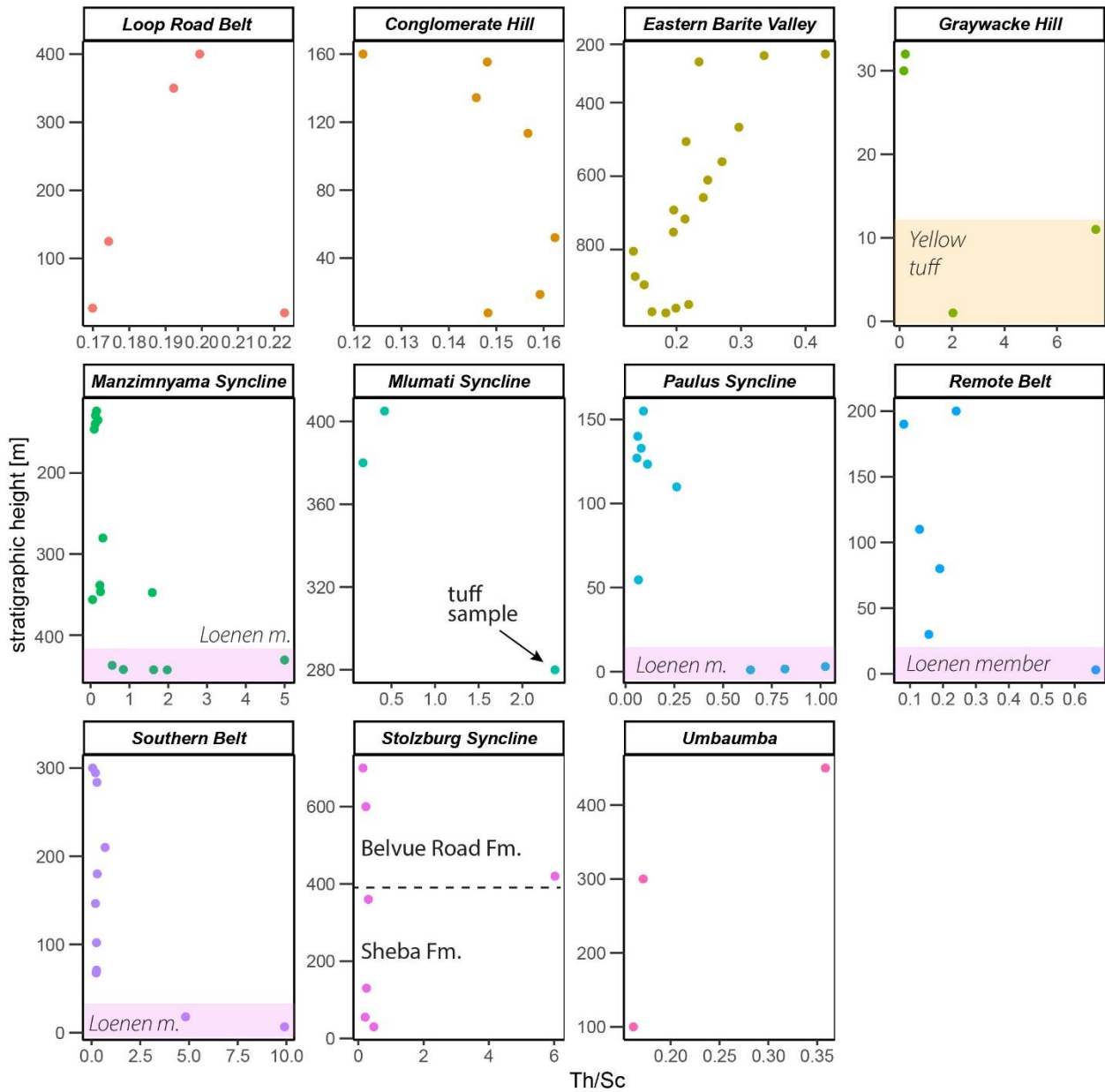
39 **Supplementary Figure 3:** Cr/Zr ratio of samples with stratigraphic control. Samples from Eastern Barite
 40 Valley and Manzimnyama Syncline are from the BARB5 and BARB4 drill cores, respectively, hence the
 41 stratigraphic height is measured in core depth. Samples from Umbaumba sequence are from Hofmann
 42 (2005) and samples from the Mlumati Syncline from Stoll et al. (2021). All structural belts represent the
 43 Mapepe Formation unless indicated. Note the changes in scale on both axes.

44



45 **Supplementary Figure 4:** Th/Sc ratio of samples with stratigraphic control. Samples from Eastern Barite
 46 Valley and Manzimnyama Syncline are from the BARB5 and BARB4 drill cores, respectively, hence the
 47 stratigraphic height is measured in core depth. Samples from Umbaumba sequence are from Hofmann
 48 (2005) and samples from the Mlumati Syncline from Stoll et al. (2021). All structural belts represent the
 49 Mapepe Formation unless indicated. Note the changes in scale on both axes.

50



51 **Supplementary Figure 5:** La_N/Yb_N ratio of samples with stratigraphic control. Samples from Eastern
 52 Barite Valley and Manzimnyama Syncline are from the BARB5 and BARB4 drill cores, respectively,
 53 hence the stratigraphic height is measured in core depth. Samples from Umbaumba sequence are from
 54 Hofmann (2005) and samples from the Mlumati Syncline from Stoll et al. (2021). Note the changes in
 55 scale on both axes.

56

